

Sonically modified zeolites with MFI and USY type structure as catalysts for methane combustion. Preparation and physicochemical characterisation

Łukasz Kuterasiński^{a,*}, Klaudia Dymek^b, Przemysław Jakub Jodłowski^{b,*}

^a Jerzy Haber Institute of Catalysis and Surface Chemistry Polish Academy of Sciences, Niezapominajek 8, 30–239 Kraków, Poland

^b Faculty of Chemical Engineering and Technology, Cracow University of Technology, Warszawska 24, 30–155 Kraków, Poland

Article history:

Received 10 September 2019

Received in revised form

29 September 2019

Accepted 30 September 2019

Available online 30 September 2019

Abstract

The objectives of our study were to prepare of ZSM-5 and USY-based catalysts by hydrothermal method, containing metallic active phase, deposited by both conventional ionic-exchange or ultrasonic irradiation. Prepared materials were characterized by various physicochemical methods, such as XRD, BET, SEM, UV-VIS and the sorption of ammonia monitored by FT-IR spectroscopy. The XRD data confirmed pure MFI or USY type structure zeolite. BET and ammonia sorption results have shown that the presented method leads to preparation of highly porous and acidic systems. Metallic active phase was found as cations and oxides with hexagonal and octahedral coordination.

Keywords: hydrothermal synthesis, zeolites, ultrasounds, methane combustion

Introduction

Methane being a basic component of natural gas, shale gas and other mine gases, is one of the most commonly used gas in order to obtain energy. It is also an important precursor for the synthesis of chemical compounds, such as methanol [1].

Previously, many systems were investigated in catalytic oxidation of methane to methanol in order to find catalysts in the presence of which the maximal both conversion of methane and yield of methanol could be found. The reaction has been studied mostly over mercury, palladium, thallium and molybdenum oxides [2], but reported catalytic results were not satisfying.

Presently, the studied catalytic systems in the reaction of selective methane oxidation are zeolitic materials, mainly CuZMS-5 and FeZMS-5 [3]. The choice of zeolites comes from their numerous advantages, such as: high specific surface area, shape-selectivity and their high susceptibility to any modifications related to chemical composition, structure, porosity, acidity or even morphology [4].

Based on a review of literature, the application of ultrasounds in the synthesis and modification of catalysts for the selective oxidation of methane seems to be a remedy for a high energy and time-consuming procedures. That implies the possibility of performance of the process under milder conditions, reducing energy expenditure or the need to use some reagents [5].

The specific properties of sonochemical irradiation were

found in numerous applications in zeolite chemistry, such as: in the synthesis of zeolites A [6], and 4A [7], MCM-22 [8], NaP [9], etc. The first study concerning ultrasound-assisted modification of zeolites was reported by Hosseini et al. [10], who investigated an ultrasound-assisted dealumination of zeolite Y in an ethanol-acetylacetone solution as a chelating agent.

In this study, we have synthesized MFI- and USY-type zeolites, containing metal active phase introduced by both conventional and sonochemical techniques. Obtained systems are intended to be used in the future as catalysts for selective oxidation of methane. The scope of work includes both preparation and characterisation of chosen materials.

Experimental

Sample preparation

MFI-type zeolite with Si/Al = 37 as well as ultrastabilised form of Y zeolite (USY) with Si/Al = 2.65 have been synthesized. For the zeolite with MFI structure, gel of defined chemical composition was obtained by several steps. At first, sodium aluminate (Avantor, p.a) was dissolved in water. Then, a silicon source (tetraethylortosilicate; 98%, Sigma-Aldrich) and a specimen (tetrapropylammonium hydroxide; 1.0 M, Sigma-Aldrich) were added to the sodium aluminate (Riedel-de Haën, 54 wt.-% Al₂O₃, 41 wt.-% Na₂O) aqueous solution under vigorous stirring and aged at room temperature for 20 h. After the ageing procedure, the gel was transferred into Teflon-lined stainless-steel rotating autoclaves (56 RPM), sealed and kept at 175°C for 20 h. After that time, the obtained systems were washed by distilled

*Corresponding author: nckutera@cyf-kr.edu.pl, jodlowski@chemia.pk.edu.pl

water and dried at 80°C in static air. In order to remove the organic residue (TPAOH) from prepared catalysts, the calcination at 480°C for 8 h with a thermal ramp of 2°C/min. was carried out. Afterwards, the specimen-free samples were being ion-exchanged three times with a 0.1 M aqueous NH_4NO_3 solution for 2 h at 80 °C. Subsequently, in order to generate protonic acid sites, dry zeolites in ammonium form were being calcined at 450°C for 8 h in dry air with thermal ramp 2°C/min. The decomposition of ammonium ions undergoes the reaction in accordance with the following formula: $\text{NH}_4^+ \rightarrow \text{H}^+$. MFI-type zeolite with Si/Al = 37 in protonic form has been denoted as HMFI37.

In case of Y-type zeolite (Si/Al=2.65), the colloidal silica (Ludox AS 40%) was added under vigorous stirring to the sodium aluminate (Riedel-de Haën, 54 wt.-% Al_2O_3 , 41 wt.-% Na_2O), previously dissolved in 2.5 M NaOH aqueous solution. The resulting gel was then transferred into a Teflon-lined stainless-steel autoclaves, sealed and kept at room temperature for 24 h and at 95°C for next 24 h in the furnace in static conditions. Synthesized systems were rinsed by distilled water and dried at 80°C in the furnace.

In order to obtain USY-type structure, the ion exchange of Y type zeolite with a 0.1 M aqueous ammonium nitrate solution at 80°C for 2 h was being performed three times. Afterwards, NH_4^+ -Y was being steamed at 700°C for 3 h with a thermal ramp of 2°C/min, with the use of saturated water vapor under 1.25 kPa pressure and with the flow of 50 cm^3/min . During heating and cooling, saturated water vapor was replaced by dry air. USY-type zeolite with Si/Al = 2.65 has been denoted as USY2.65.

Finally, prepared catalysts were being ion-exchanged in 0.5 M aqueous copper or cobalt nitrate as well as with the use of 5 mM aqueous iron or chromium nitrate solutions (Sigma-Aldrich) at 20°C for 24 h. For comparison, the introduction of metallic active phase within zeolitic structure was performed in the presence of ultrasounds. In the sonochemical method, the obtained zeolites were immersed in aqueous metal nitrate solutions (described above) and were being sonochemically treated for 20 min at room temperature, using QSonica S-4000 sonicator equipped with a 1/2 diameter horn (average power of sonication was 60 W and frequency 20 kHz). During the sonication procedure, the glass tube filled with the catalyst precursors was placed in ice bath. Directly before sonication, the samples were outgassed for 15 min. using argon (Linde Gaz Polska Sp. z o. o., 99.5%) with flow rate of 20 cm^3/min , and 1.5 mL of ethanol was added to the suspension.

Subsequently, Cu/Co/Fe/Cr containing samples were washed with distilled water three times and dried. The metal-zeolites were being calcined in dry air for 4 h at 500°C with thermal ramp of 2 °C/min and flow rate of 50 cm^3/min .

Sample characteristics

The XRD measurements were being performed at room temperature with diffractometer PANalytical X'Pert PRO MPD with

$\text{CuK}\alpha$ radiation ($\lambda=1.5418 \text{ \AA}$) at 40 kV and 30 mA and over 20 range from 5 to 50° with 0.033° step every 12 min. The zeolite samples subjected to research were placed in holders in powder form.

Porous structure was investigated by N_2 physisorption at -196°C using Quantachrome Nova 2000. Prior to the experiment, the samples were activated in vacuum at 300°C for 20 h. Surface Area (S_{BET}) and micropore volume (V_{micro}) were determined with the use of BET and t-plot methods, respectively. Pore size distribution and meso- and micropores volume (V_{meso} , V_{micro}) were calculated by the application of Barrett-Joyner-Halenda (BJH) model to the adsorption branch of the isotherm. The accuracy of these measurements was ca. 10%.

The morphology of the prepared samples was determined by scanning electron microscopy, using a JEOL 5400 scanning microscope (JEOL USA, Inc., Peabody, MA, USA) with a LINK ISIS microprobe analyser (Oxford Instruments, Tubney Woods Abingdon, Oxfordshire, UK). Prior to analysis, the samples were being dried for 24 hours and covered with a carbon layer.

The FT-IR spectra were recorded using Nicolet is10 spectrometer with MCT detector from Thermo Scientific. The scanning range was 650 - 4000 cm^{-1} with resolution of 4 cm^{-1} , and 100 scans per each spectrum. Prior to IR studies, the samples were pressed into thin self-supported wafers and activated in vacuum at 400°C for 1 h with a thermal ramp of 5°C/min. After activation, the reference spectrum was recorded at 120°C. NH_3 (Air Products 99.95%) was distilled by freeze/thaw cycles before adsorption to remove any traces of moisture and impurities and then adsorbed on the surface of sample at 120°C. The amount of probe molecules introduced into the IR cell was calculated from the ideal gas law. The concentration of Brønsted and Lewis sites was calculated from the intensities of 1450 cm^{-1} and 1620 cm^{-1} bands assigned to ammonium ion (NH_4^+) and ammonia interacting with Lewis sites (NH_3L) and their extinction coefficients equal to 0.12 and 0.026 $\text{cm}^2/\mu\text{mol}$, respectively.

UV-VIS Diffuse Reflectance Spectra (UV-VIS DRS) were obtained using AvaSpec-ULS3648 High-resolution spectrometer equipped with a Praying Mantis High-Temperature Reaction Chamber (Harrick Scientific Co., Ossining, NY) and a high-temperature reflection probe (FCR-7UV400-2-ME-HTX, 7 400 μm fibers). The AvaLight-D(H)-S Deuterium-Halogen was used as the light source. The spectra were recorded in the frequency range of 200-1000 nm. The instrument was controlled by AvaSoft v 9.0 software. The spectra were recorded after dehydration at 110°C in a helium flow (30 cm^3/min).

Results and discussion

XRD

The X-ray diffraction (XRD) patterns for both pure zeolites (HMFI37 and USY2.65) and Cu or Co or Fe or Cr modified catalysts prepared via classical ion exchange or sonochemical tech-

nique are presented in Figure 1. The analysis of the diffraction reflexes for all samples was performed based on the American Mineralogist Crystal Structure Database [11]. The analysis indicated the presence of MFI- and USY-type zeolites for both raw and metal containing samples. For MFI and USY-type zeolites, the introduction of Cu, Co, Fe and Cr within zeolitic structure did not alter the appearance of XRD patterns. One exception was USY2.65 modified with Cr by both ion-exchange and sonochemical method, for which the collapse of crystalline structure was found (Fig. 1 c, 1d). Observed feature may be explained by very low pH (≈ 1) of used aqueous chromium solution, which might lead to uncontrolled dealumination followed by the amorphisation of USY-type zeolite.

SEM

Scanning electron microscopy technique (SEM) was used for examination of the morphology of prepared catalysts (Fig. 2, 3). The SEM images were obtained in backscattered electron mode (BSE). In all cases, USY- and MFI-based grains are of spherical-like shape [22]. The appearance of SEM images depends neither on zeolitic structure type nor the kind of metallic phase and the method of its deposition over zeolitic support.

BET

The details concerning porosity of the studied zeolites with MFI-type structure are presented in Table 1.

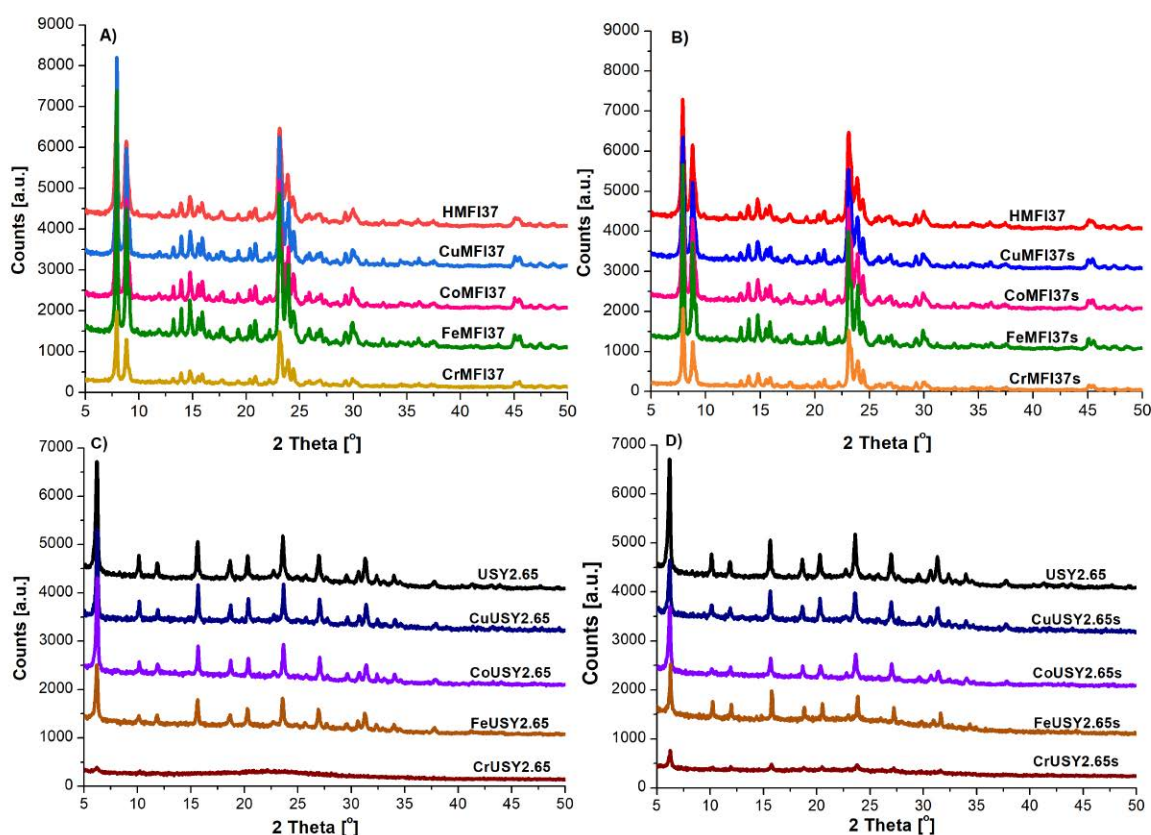


Figure 1. Diffractograms of the copper- cobalt-, iron- and chromium-substituted zeolites: (A) MFI37 samples modified by ion-exchange method; (B) MFI37 samples modified by sonochemical technique; (C) USY2.65 samples modified by ion-exchange method; (D) USY2.65 samples modified by sonochemical technique

Neither XRD patterns of Cu/Co/Fe/Cr oxides nor Cu/Co/Fe/Cr hydroxides were found in all prepared zeolitic samples. It may be concluded that the incorporated metal species are uniformly distributed within zeolitic structure as cations exchanging the $-OH$ groups connected to Al. Furthermore, after metal introduction, there is always some fraction of the residual oxides or hydroxides in the form of crystallites that occur over external surface of zeolitic grains [11–14].

The results of specific surface areas determined by sorption of N_2 for the raw HMF1 was slightly smaller in relation to the metal loaded samples. Generally, the specific surface area for the Cu/Co/Fe/Cr-containing zeolites slightly increased e.g. for CuMFI37 and CoMFI37 samples it reached the values of $369 \text{ m}^2/\text{g}$ and $337 \text{ m}^2/\text{g}$, respectively, while for HMF1 zeolite the specific surface area was $328 \text{ m}^2/\text{g}$ (Table 1). A similar observation can be made when comparing the mesoporous volume results and average pore diameter. The mesoporous volume and average pore diameter measured for the pure HMF137, were equal to $0.095 \text{ cm}^3/\text{g}$ and 26.7 \AA , respectively. In turn, for the Cu- and Cr-

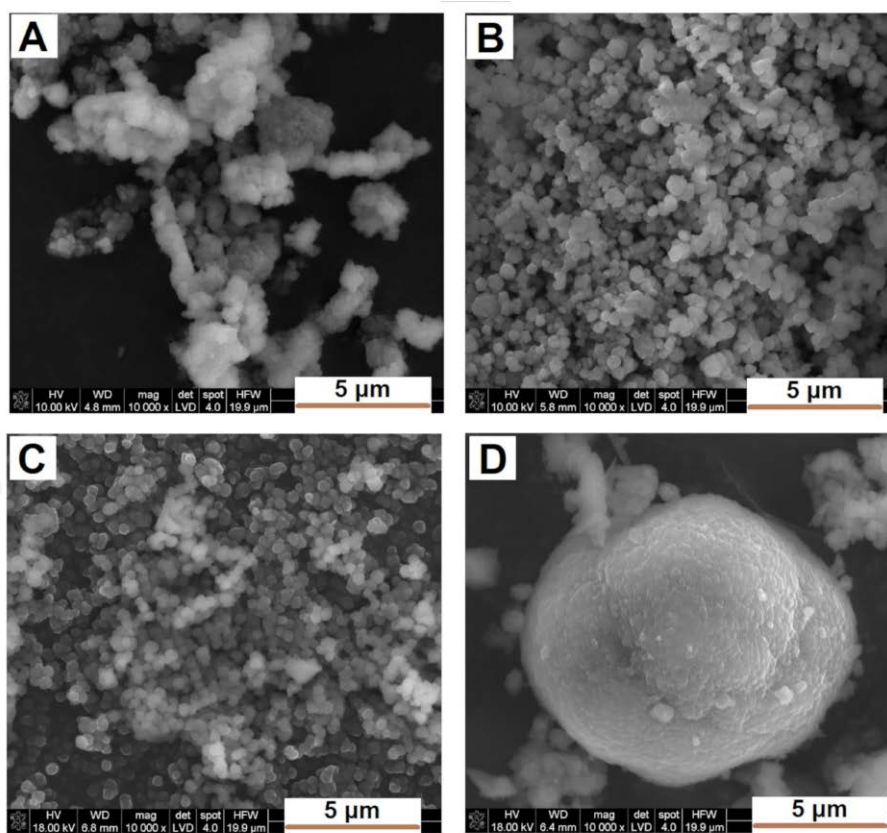


Figure 2. Scanning electron microscopy (SEM) images of MFI-37-type zeolite samples (5 μm): (A) CuMFI37; (B) CuMFI37s; (C) FeMFI37; (D) FeMFI37s.

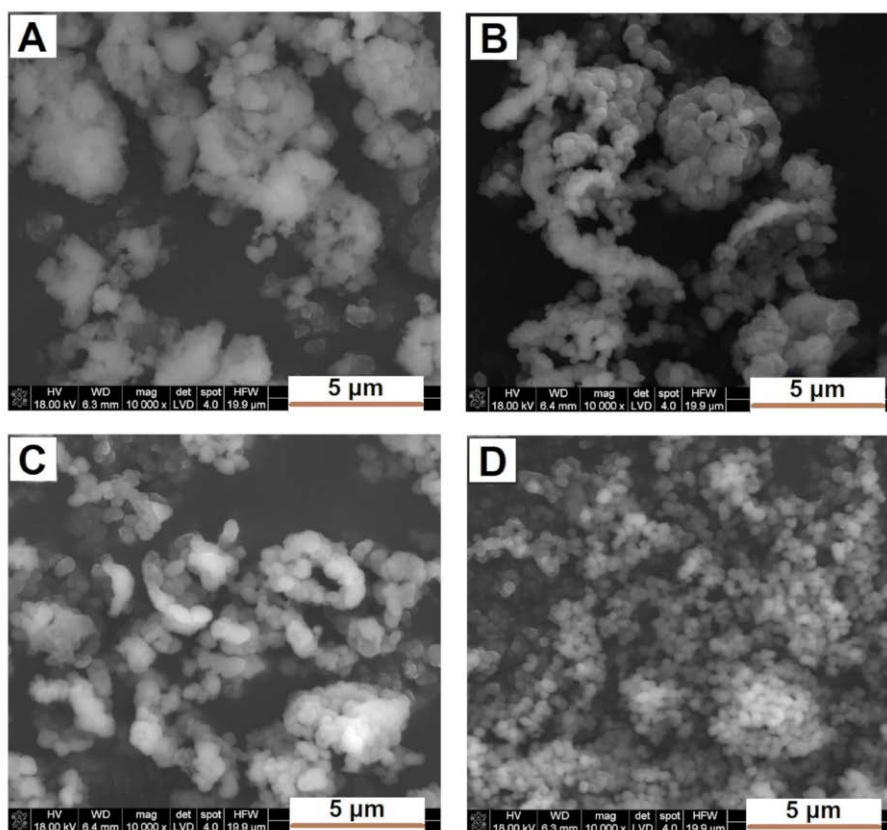


Figure 3. Scanning electron microscopy (SEM) images of USY2.65-type zeolite samples (5 μm): (A) CuUSY2.65; (B) CuUSY2.65s; (C) FeUSY2.65; (D) FeUSY2.65s.

containing samples mesoporous volume increased considerably, to 0.268 and 0.153 cm³/g, respectively. For metal-containing zeolites, average pore diameter reached 40.2 Å (CuMFI37). An opposite effect was observed in the case of microporous volume, which may be related to blocking of micropores by metal species [15].

trasonic modification, these values were equal to: 337 m²/g, 386 m²/g, 373 m²/g and 28 m²/g, respectively. A similar trend was found for microporous volume results. The microporous pore volume measured for the pure zeolite USY, was equal to 0.182 cm³/g, whereas for the Cu-, Co-, Fe and Cr- containing samples it decreased to 0.142 cm³/g, 156 cm³/g, 0.106 and 0.002 cm³/g, respectively. A possible explanation for those decreases found

Table 1. Porous structure and acidity of Cu/Co/Fe/Cr containing MFI37-type zeolites

Sample	Si/Al	S _{BET} [m ² /g]	V _{micro} [cm ³ /g]	V _{meso} [cm ³ /g]	D [Å]	BAS [μmol/g]	LAS [μmol/g]
HMFI37	37	328	0.124	0.095	26.7	435	31
CuMFI37	37	369	0.103	0.268	40.2	173	225
CuMFI37s	37	359	0.104	0.242	38.6	220	148
CoMFI37	37	326	0.108	0.132	29.5	152	206
CoMFI37s	37	358	0.107	0.246	39.4	260	58
FeMFI37	37	321	0.096	0.159	25.5	123	80
FeMFI37s	37	337	0.103	0.133	28.1	263	79
CrMFI37	37	337	0.117	0.153	32.1	210	45
CrMFI37s	37	372	0.125	0.165	31.1	352	26

The results of porous structure showed some correlation between the kind of introduced metal within zeolitic structure. For Cu- and Co-containing catalysts, porosity has changed more significantly than for Fe- and Cr-counterparts. For MFI-type catalysts, the modification with Cu/Co/Fe/Cr both by ion-exchange or sonochemical method led to comparable changes in the structure of pores.

The data referring to porosity of USY-type zeolites are given in Table 2. In the case of USY-based samples, specific surface area of raw USY2.65 zeolite was higher (450 m²/g) in comparison to the cation exchanged samples. For USY-based catalysts, modified with Cu, Co, Fe and Cr both by ion-exchange and ul-

for the USY catalysts can be the blocking of the pore system by metal oxides that can be formed upon modification [15]. For USY-based catalysts, the incorporation of Cu, Co and Fe within zeolitic structure both by ion-exchange or sonochemical technique caused similar changes in porosity of modified materials.

The results of porosity did not show relevant correlation between the kind of introduced metal. One exception was Cr containing USY zeolite, for which all presented values clearly differed from the rest of samples, e.g. for CrUSY2.65 sample, the specific surface area and microporous volume values decreased from 450 m²/g to 28 m²/g and from 0.182 cm³/g to 0.002 cm³/g, respectively. At the same time, an enormous increase of average

Table 2. Porous structure and acidity of Cu/Co/Fe/Cr containing USY2.65-type zeolites

Sample	Si/Al	S _{BET} [m ² /g]	V _{micro} [cm ³ /g]	V _{meso} [cm ³ /g]	D [Å]	BAS [μmol/g]	LAS [μmol/g]
USY2.65	2.65	450	0.182	0.198	33.8	n.d.	n.d.
CuUSY2.65	2.65	337	0.142	0.160	35.9	24	261
CuUSY2.65s	2.65	382	0.150	0.203	37.0	14	173
CoUSY2.65	2.65	386	0.156	0.219	38.8	33	43
CoUSY2.65s	2.65	379	0.139	0.217	37.5	50	169
FeUSY2.65	2.65	373	0.106	0.277	41.1	n. d	n. d.
FeUSY2.65s	2.65	300	0.085	0.210	39.3	n. d	n. d.
CrUSY2.65	2.65	28	0.002	0.111	159.3	125	143
CrUSY2.65s	2.65	278	0.085	0.153	34.2	133	91

pore diameter from 33.8 Å to 159.3 Å was found for this sample, which may be explained by the amorphisation of such modified USY-type zeolite. These results are in accordance with XRD analysis (Fig. 1).

Acid properties

The results concerning the nature and concentration of the active sites present in MFI- and USY-based catalysts, determined by NH_3 chemisorption are presented in Table 1 and 2.

The comparison of the concentration of Brønsted acid sites within studied samples led to the conclusion that prepared samples revealed significant differences in acidity. For MFI zeolites, the concentration of Brønsted acid sites varied between 123–450 $\mu\text{mol/g}$, whereas for USY-based catalysts this value was significantly lower, and varied between 14–133 $\mu\text{mol/g}$. Aluminosilicates characterised by low Si/Al ratio (like X, Y, A type zeolites) are more prone to dehydroxylation of acid OH groups existing in close vicinity, that leads to the formation of Lewis acid sites assigned to aluminum species [16–18]. For MFI-type samples, the incorporation of Cu/Co/Fe/Cr species resulted in significant decrease of the concentration of Brønsted acid sites with simultaneous increase of the concentration of Lewis acid sites. Furthermore, it was found that for the samples modified by ion-ex-

change method, the decrease of the concentration of Brønsted acid sites was more evident in comparison to analogues treated with ultrasounds irradiation.

The detailed analysis of the Lewis acidity allows us to claim that the concentration of this type of acid sites corresponds both with the valence of the cationic form of metal incorporated into zeolitic structure and the concentration of aqueous metal salt solution used during the treatment. For all studied samples (both MFI and USY type zeolites), the presence of Cu or Co species (mainly as Cu^{2+} and Co^{2+}) resulted in distinct higher concentration of Lewis acid sites, particularly for Cu containing samples [19–21]. In the case of Fe- and Cr-analogues, lower concentration of Lewis acid sites in comparison to Cu and Co counterparts probably comes from the utilization of hundredfold diluted aqueous solutions of Fe and Cr salts during modification of zeolites.

UV-VIS

The UV-VIS DRS spectra of the metal containing samples are presented in Figure 4. For Cu-samples (Fig.4a), the band at 256 nm may be assigned to Cu^{2+} interacting with oxygen atoms in the zeolitic structure (charge transfer $\text{O} \rightarrow \text{Cu}$ transmission). In turn, the band between 550 and 1000 nm with maximum at ca 850 nm might come from CuO [22–23].

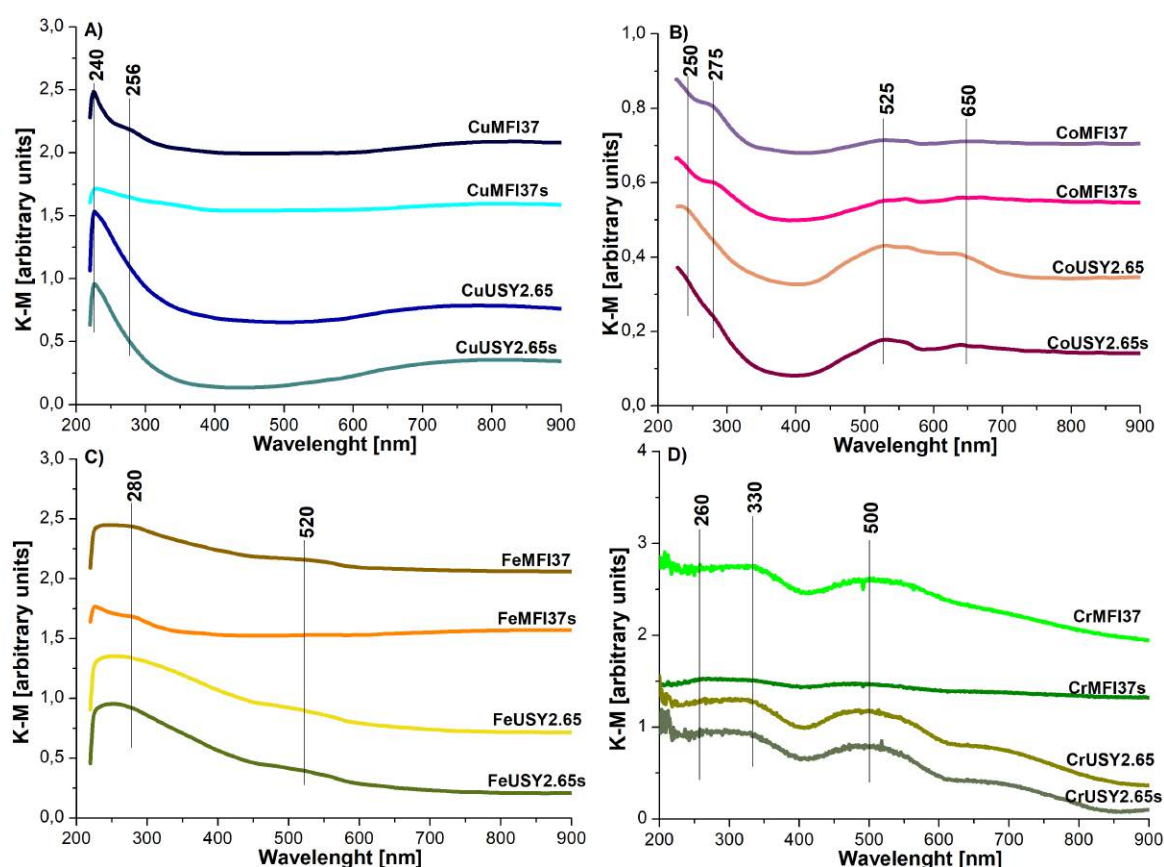


Figure 4. In situ diffuse reflectance UV/visible (UV/Vis) spectra of prepared metal-substituted zeolites: (A) CuMFI37, CuMFI37s, CuUSY2.65, CuUSY2.65s catalysts; (B) CoMFI37, CoMFI37s, CoUSY2.65, CoUSY2.65s catalysts; (C) FeMFI37, FeMFI37s, FeUSY2.65, FeUSY2.65s catalysts; (D) CrMFI37, CrMFI37s, CrUSY2.65, CrUSY2.65s catalysts

In the UV-VIS DRS spectra of Co-catalysts (Fig. 4b), the maxima at 250 and 275 nm is attributed to Co^{2+} compensating the negative charge of the zeolite and oxygen-to-metal charge transfer (CT) transition, respectively. The broad band at with maximum at 525 nm may correspond to Co_3O_4 [22], while the broad signal with maximum at 650 nm might come from surface $\text{Co}^{2+}/\text{Co}^{3+}$ species [24]. Furthermore, the maxima at ca 550 and 650 nm may be attributed to isolated tetrahedral Co(II) species and associated with ${}^4\text{A}_2 \rightarrow {}^4\text{T}_1$ (4P) and ${}^4\text{A}_2 \rightarrow {}^4\text{T}_2$ transitions, respectively [13].

In the UV-VIS DRS spectra of Fe containing samples (Fig. 4c), the band at 280 nm may correspond to Fe^{3+} in octahedral coordination. In turn, the broad band with maximum at 520 nm may be attributed to Fe_2O_3 [25].

In the case of Cr-samples (Fig.4d), the bands with maxima at 260 and 330 nm may be assigned to Cr^{6+} interacting with oxygen atoms in the zeolitic structure (charge transfer $\text{O} \rightarrow \text{Cr}$ transmission), which may be illustrated as: $(\text{O}^{2-}=\text{Cr}^{6+})-(\text{Cr}^{5+}-\text{O}^{-1})$ [26]. In turn, the band with maximum at 500 nm is probably attributed to Cr_xO_y species.

Conclusions

In this research, we presented the synthesis of MFI and USY zeolites by hydrothermal method, followed by the introduction of metallic active phase in the form of copper, cobalt, iron and chromium species, both by ionic-exchange and sonochemical technique. The physicochemical properties of the samples obtained in this way were investigated. We have focused on the influence of the type of zeolitic structure as well as the kind of introduced metal into the zeolitic carrier on the topology, porous structure, morphology, the form of active phase and acidity of prepared systems.

The analysis of the obtained data led to the following conclusions:

- The analysis of XRD patterns confirmed the presence of MFI and USY zeolitic structures for both raw and ion-exchanged samples. In all cases, neither XRD patterns of Cu/Co/Fe/Cr oxides nor Cu/Co/Fe/Cr hydroxides were found, which can be explained by the fact that the incorporated metallic species are uniformly distributed within the zeolite structure.
- The results of specific surface areas and total pore volumes did not show relevant correlation both between the kind of the structure of the support and the type of metal introduced into zeolite. One exception was zeolite USY modified with Cr, for which the specific surface area and microporous volume values decreased from $450 \text{ m}^2/\text{g}$ to $28 \text{ m}^2/\text{g}$ and from $0.182 \text{ cm}^3/\text{g}$ to $0.002 \text{ cm}^3/\text{g}$, respectively. At the same time, an enormous increase of average pore diameter from 33.8 \AA to 159.3 \AA was found for this sample, which can be explained by the amorphisation of such modified USY-type zeolite.
- The results referring to the nature of the active sites present

in the prepared samples, determined by NH_3 chemisorption indicated that the concentration both of Brønsted and Lewis acid sites depends strictly on the topology of zeolitic carrier (coming from Si/Al ratio) as well as on the kind of the metal introduced within zeolitic structure. Furthermore, it was concluded that the application of sonochemical method for the deposition of metallic compounds onto zeolite resulted in higher concentrations of Brønsted acid sites in comparison with the samples modified by conventional way.

- UV-VIS analysis allowed us to determine the status of the active phase, which was present within zeolitic structure. Copper, cobalt, iron and chromium were found as cations and oxides with hexagonal and octahedral coordination.
- All prepared and characterised systems will be studied as catalysts in the reaction of methane combustion.

Acknowledgement

The Project was financed by National Centre for Research and Development No. LIDER/204/L-6/14/NCBR/2015.

References

1. Khirsariya P, Mewada RK: Single step oxidation of methane to methanol – towards better understanding. *Procedia Eng.* 2013; 51: 409–415.
2. Jones C, Taube D, Ziatdinov VR, Periana RA, Nielsen RJ, Osgaard J, Goddard W: Selective oxidation of methane to methanol catalyzed with C-H activation by homogeneous cationic gold. *Angew. Chem. Int. Ed. Engl.* 2004; 6: 4626–4629.
3. Xiao P, Wang Y, Nishitoba T, Kondo JN, Yokoi T: Selective oxidation of methane to methanol with H_2O_2 over Fe-MFI zeolites catalyst using sulfone solvent. *Chem. Commun.* 2019; 55: 2896–2899.
4. Kierys A, Goworek J: Adsorbenty i Katalizatory. Wybrane technologie a środowisko, w Materiały krzemionkowe nowej generacji, Uniwersytet Rzeszowski, 2012. http://www.ztch.umcs.lublin.pl/materiały/praca_zbiorowa_wprowadzenie.pdf
5. Bonrath W: Ultrasound supported catalysis. *Ultrason. Sonochem.* 2005; 12: 103–106.
6. Andac O, Tatlier M, Sirkecioglu A, Ece I, Erdem-Senatalar A: Effects of ultrasound on zeolite A synthesis. *Microporous Mesoporous Mater.* 2005; 79: 225–233.
7. Andac O, Murat Telli S, Tatlier M, Erdem-Senatalar A: Effects of ultrasound on the preparation of zeolite A coatings. *Microporous Mesoporous Mater.* 2006; 88: 72–76.
8. Wang B, Wu J, Yuan ZY, Li N, Xiang S: Synthesis of MCM-22 zeolite by an ultrasonic-assisted aging procedure. *Ultrason. Sonochem.* 2008; 15: 334–338.
9. Pal P, Das JK, Das N, Bandyopadhyay S: Synthesis of NaP zeolite at room temperature and short crystallization time by sonochemical method. *Ultrason. Sonochem.* 2013; 20: 314–321.

10. Hosseini M, Zanjanchi MA, Ghalami-Chooabar B, Golmojdeh H: Ultrasound-assisted dealumination of zeolite Y. *J. Chem.* 2015; 127: 25–31.
11. Pereda-Ayo B, De La Torre U, JoséIllán-Gómez M, Bueno-López A, González-Velasco JR: Role of the different copper species on the activity of Cu/zeolite catalysts for SCR of NO_x with NH₃. *Appl. Catal. B.* 2014; 147: 420–428.
12. Yan JY, Lei GD, Sachtler WMH, Kung HH: Deactivation of Cu/ZSM-5 catalysts for lean NO_x reduction: Characterization of changes of Cu state and zeolite support. *J. Catal.* 1996; 161: 43–54.
13. Janas J, Machej T, Gurgul J, Socha RP, Che M, Dzwigaj S: Effect of Co content on the catalytic activity of CoSiBEA zeolite in the selective catalytic reduction of NO with ethanol: Nature of the cobalt species. *Appl. Catal. B.* 2007; 75: 239–248.
14. Li LD, Shen Q, Yu JJ, Hao ZP, Xu ZP, Lu GQM: Fe-USY zeolite catalyst for effective decomposition of nitrous oxide. *Environ. Sci. Technol.* 2007; 41: 7901–7906.
15. Lee K, Kosaka H, Sato S, Yokoi T, Choi B, Kim D: Effects of Cu loading and zeolite topology on the selective catalytic reduction with C₃H₆ over Cu/zeolite catalysts. *J. Industrial and Eng. Ch.* 2019; 72: 73–86.
16. Datka J, Kawałek M: Strength of Brønsted acid sites in boralites. *J. Chem. Soc. Faraday Trans.* 1993; 89: 1829–1831.
17. Yashmina T, Yamazaki K, Ahmad H, Katsuta M, Hara N: Alkylation on synthetic zeolites: II. Selectivity of p-xylene formation. *J. Catal.* 1970; 17: 151–156.
18. Freude D, Frochlich T, Hunger M, Pfeifer H, Scheler G: NMR studies concerning the dehydroxylation of zeolites HY. *Chem. Phys. Lett.* 1983; 98: 263–266.
19. Brylewska K, Tarach KA, Mozgawa W, Olejniczak Z, Filek U, Góra-Marek K: Modification of ferrierite through post-synthesis treatments. Acidic and catalytic properties. *J. Mol. Struct.* 2016; 1126: 147–153.
20. Chmielarz L, Kuśtrowski P, Zbroja M, Gil-Knap B, Datka J, Dziembaj R: SCR of NO by NH₃ on alumina or titania pillared montmorillonite modified with Cu or Co Part II. Temperature programmed studies. *Appl. Catal. B.* 2004; 53: 47–61.
21. Rutkowska M, Diaz U, Palomares AE, Chmielarz L: Cu and Fe modified derivatives of 2D MWW-type zeolites (MCM-22, ITQ-2 and MCM-36) as new catalysts for DeNO_x process. *Appl. Catal. B.* 2015; 168–169: 531–539.
22. Urquieta-Gonzales EA, Pequin RPS, Batiste MS: Identification of extra-framework species on Fe/ZSM-5 and Cu/ZSM-5 catalysts typical microporous molecular sieves with zeolitic structure. *Materials Research.* 2002; 5: 321–327.
23. Shen Q, Li L, He C, Zhang X, Hao Z, Xu Z: Cobalt zeolites: Preparation, characterization and catalytic properties for N₂O decomposition. *Asia-Pac. J. Chem. Eng.* 2012; 7: 502–509.
24. Xie P, Luo Y, Ma Z, Wang L, Huang C, Yue Y, Hua W, Gao Z: CoZSM-11 catalysts for N₂O decomposition: Effect of preparation methods and nature of active sites. *Appl. Catal. B.* 2015; 170: 34–42.
25. Chlebda DK, Stachurska P, Jędrzejczyk RJ, Kuterasiński Ł, Dziedzicka A, Górecka S, Chmielarz L, Łojewska J, Sitarz M, Jodłowski PJ: DeNO_x abatement over sonically prepared iron substituted Y, USY and MFI zeolite catalysts in lean exhaust gas conditions. *Nanomaterials.* 2018; 8: 21–39.
26. Zhao Z, Duan A, Xu C: CrHZSM-5 zeolites- highly efficient catalysts for catalytic cracking of isobutane to produce light olefins. *Catal. Lett.* 2006; 109: 65–70.